A chemical-genetic approach to study G protein regulation of β cell function in vivo

Jean-Marc Guettier[a,1], Dinesh Gautam[a], Marco Scarselli[a,2], Inigo Ruiz de Azua[a], Jian Hua Li[a], Erica Rosemond[a], Xiaochao Ma[b,3], Frank J. Gonzalez[b], Blaine N. Armbruster[c,4], Huiyan Lu[d], Bryan L. Roth[c], and Jürgen Wess[a,1]

[a]Molecular Signaling Section, Laboratory of Bioorganic Chemistry, National Institute of Diabetes and Digestive and Kidney Diseases, [b]Laboratory of Metabolism, National Cancer Institute, and [d]Mouse Transgenic Core Facility, National Institute of Diabetes and Digestive and Kidney Diseases, National Institutes of Health, Bethesda, MD 20892; and [c]Department of Pharmacology and Division of Medicinal Chemistry and Natural Products, University of North Carolina Chapel Hill Medical School, Chapel Hill, NC 27514

Edited by Robert J. Lefkowitz, Duke University Medical Center/Howard Hughes Medical Institute, Durham, NC, and approved September 11, 2009 (received for review June 16, 2009)

Impaired functioning of pancreatic β cells is a key hallmark of type 2 diabetes. β cell function is modulated by the actions of different classes of heterotrimeric G proteins. The functional consequences of activating specific β cell G protein signaling pathways in vivo are not well understood at present, primarily due to the fact that β cell G protein-coupled receptors (GPCRs) are also expressed by many other tissues. To circumvent these difficulties, we developed a chemical-genetic approach that allows for the conditional and selective activation of specific β cell G proteins in intact animals. Specifically, we created two lines of transgenic mice each of which expressed a specific designer GPCR in β cells only. Importantly, the two designer receptors differed in their G protein-coupling properties ($G_{q/11}$ versus G_s). They were unable to bind endogenous ligand(s), but could be efficiently activated by an otherwise pharmacologically inert compound (clozapine-N-oxide), leading to the conditional activation of either β cell $G_{q/11}$ or G_s G proteins. Here we report the findings that conditional and selective activation of β cell $G_{q/11}$ signaling in vivo leads to striking increases in both first- and second-phase insulin release, greatly improved glucose tolerance in obese, insulin-resistant mice, and elevated β cell mass, associated with pathway-specific alterations in islet gene expression levels. Selective stimulation of β cell G_s triggered qualitatively similar in vivo metabolic effects. Thus, this developed chemical-genetic strategy represents a powerful approach to study G protein regulation of β cell function in vivo.

beta cells | G protein-coupled receptors | transgenic mice | type 2 diabetes

Type 2 diabetes has emerged as one of the major threats to human health in the 21st century (1). Impaired function of pancreatic β cells is one of the key hallmarks of type 2 diabetes, and therapies targeted at improving β cell function are predicted to offer considerable therapeutic benefit (2).

β Cell function is modulated by the actions of different classes of heterotrimeric G proteins which are the immediate downstream targets of a multitude of G protein-coupled receptors (GPCRs). Like most other cell types, pancreatic β cells are predicted to express many different GPCRs (3–5). Several lines of evidence suggest that activation of G_s-coupled receptors expressed by pancreatic β cells, including the glucagon-like peptide (GLP-1) receptor, improves β cell function and can increase in β cell mass via cAMP-dependent mechanisms (5–7). Pancreatic β cells also express several $G_{q/11}$-coupled receptors, including the M_3 muscarinic acetylcholine (ACh) receptor (M3R) and GPR40, which can promote insulin release in an agonist-dependent fashion [for recent reviews, see (5, 8)].

Studies with GLP-1 receptor agonists have yielded detailed information about the beneficial effects of G_s signaling on β cell function and whole body glucose homeostasis (note that the GLP-1 receptor is enriched in pancreatic β cells) (5–7). In contrast, much less is known about the in vivo metabolic consequences of β cell $G_{q/11}$ signaling, primarily due to the lack of receptor subtype-selective agonists and the widespread expression of most $G_{q/11}$-coupled receptors (4). For example, it remains unknown whether chronic stimulation of β cell $G_{q/11}$ signaling can lead to enhanced β cell mass, as has been reported for the G_s-coupled GLP-1 receptor (5–7). Moreover, studies with M3R (9) and GPR40 (10) mutant mice have led to conflicting results regarding the metabolic consequences of chronic activation of β cell $G_{q/11}$ signaling.

To better understand the metabolic consequences and the underlying molecular mechanisms of activating specific β cell G protein signaling pathways in vivo, the availability of an experimental system in which specific G protein families can be activated in a β cell-specific and temporally controlled fashion would be highly desirable. To address this issue, we developed a chemical-genetic strategy that allows for the conditional and selective activation of distinct β cell G proteins in intact animals. Specifically, we created two lines of transgenic mice each of which expressed a specific designer GPCR (at similar expression levels) in β cells only. Importantly, the two M3R-based receptors differed in their G protein-coupling properties ($G_{q/11}$ versus G_s). The two designer receptors could be efficiently activated by clozapine-N-oxide (CNO), an otherwise pharmacologically inert compound (11, 12), but not by ACh, the endogenous M3R ligand. As a result, CNO treatment of the transgenic mice led to the activation of β cell $G_{q/11}$ or G_s signaling pathways in vivo, in a conditional and β cell-selective fashion.

Our findings demonstrate that this chemical-genetic approach represents a powerful tool to study the functional roles of distinct G protein pathways in regulating β cell function in vivo.

Results

Generation of CNO-Sensitive Designer GPCRs with Distinct G Protein-Coupling Properties. The rat M3R was subjected to distinct mutational modifications to obtain mutant receptors that no longer respond to the endogenous ligand, ACh, but can be activated by CNO, a pharmacologically inert metabolite of the antipsychotic drug, clozapine. We generated two M3R-based mutant receptors,

Author contributions: J.-M.G., D.G., M.S., I.R.d.A., J.H.L., E.R., X.M., F.J.G., H.L., and J.W. designed research; J.-M.G., D.G., M.S., I.R.d.A., J.H.L., E.R., X.M., and H.L. performed research; B.N.A. and B.L.R. contributed new reagents/analytic tools; J.-M.G., D.G., M.S., I.R.d.A., J.H.L., E.R., X.M., and F.J.G. analyzed data; and J.-M.G. and J.W. wrote the paper.

The authors declare no conflict of interest.

This article is a PNAS Direct Submission.

Freely available online through the PNAS open access option.

[1]To whom correspondence may be addressed. E-mail: guettierj@mail.nih.gov or jwess@helix.nih.gov.

[2]Present address: Ecole Polytechnique Fédérale de Lausanne, Laboratory of Nanoscale Biology, Lausanne, Switzerland.

[3]Present address: Department of Pharmacology, Toxicology and Therapeutics, The University of Kansas Medical Center, Kansas City, KS 66160.

[4]Present address: Millipore Drug Discovery Division, Millipore Corporation, St. Charles, MO 63304.

This article contains supporting information online at www.pnas.org/cgi/content/full/0906593106/DCSupplemental.

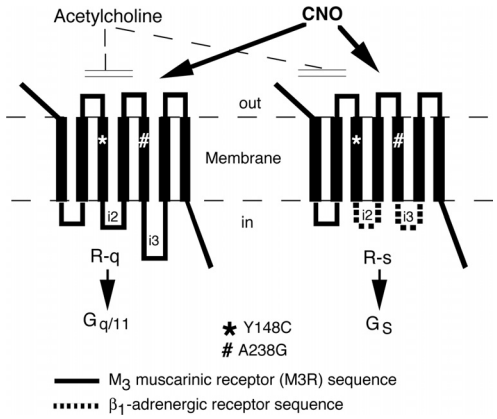

Fig. 1. Schematic representation of the structures of the R-q and R-s designer receptors. The Y148C and A238G point mutations (rat M3R sequence) were introduced into the third and fifth transmembrane domains of the two receptors. These two point mutations prevent the binding of ACh, the endogenous M3R ligand (11). However, both R-q and R-s can be activated by CNO, an otherwise pharmacologically inert compound, with high potency and efficacy. Functional studies showed that CNO binding to R-q and R-s leads to the selective activation of $G_{q/11}$ and G_s, respectively (see text for details). Note that the Y148C and A238G point mutations (rat M3R sequence) correspond to the Y149C and A239G point mutations in the human M3R (11).

referred to as R-q and R-s (Fig. 1), which selectively coupled to G proteins of the $G_{q/11}$ family and to G_s, respectively (see below).

Ligand Binding and G Protein-Coupling Properties of R-q and R-s. We initially characterized the ligand binding and functional properties of R-q and R-s in transiently transfected COS-7 cells (*SI Appendix*, Table S1 and Fig. S1). Importantly, [^{3}H]-N-methylscopolamine ([^{3}H]NMS) competition binding studies demonstrated that R-q and R-s lost the ability to bind the endogenous M3R agonist, ACh, but displayed significantly higher affinity for CNO (17- and 102-fold, respectively) than for the wild-type (WT) mouse M3R (mM3R) (*SI Appendix*, Table S1).

Functional studies showed that CNO treatment of R-q-expressing cells led to a pronounced increase in intracellular inositol phosphate (IP) levels (CNO EC_{50} value: 16.7 ± 5.3 nM; $n = 3$), consistent with the known preference of R-q for $G_{q/11}$ (11). On the other hand, CNO was essentially inactive at the WT mM3R (*SI Appendix*, Fig. S1*A*). We obtained very similar results when we studied CNO-induced increases in intracellular calcium levels (*SI Appendix*, Fig. S2), another response mediated by activated $G_{q/11}$. CNO-mediated activation of R-q did not lead to any significant changes in intracellular cAMP levels (*SI Appendix*, Fig. S1*E*), indicating that R-q neither activates nor inhibits G_s. In contrast, CNO treatment of R-s-expressing cells had virtually no effect on intracellular IP production (*SI Appendix*, Fig. S1*B*) or calcium accumulation (*SI Appendix*, Fig. S2), but led to a potent and robust increase in intracellular cAMP levels (CNO EC_{50} value: 7.4 ± 1.6 nM; $n = 3$) (*SI Appendix*, Fig. S1*F*). Addition of CNO to cells expressing the WT mM3R had no effect on intracellular cAMP levels (*SI Appendix*, Fig. S1*E*). These observations indicate that R-q and R-s selectively couple to $G_{q/11}$ and G_s, respectively. Importantly, ACh had virtually no activity at R-q and R-s in any of the second messenger assays used (*SI Appendix*, Figs. S1 *C*, *D*, *G*, *H* and S2).

SI Appendix, Fig. S1 *I* and *J* shows that CNO-mediated activation of R-q and R-s was characterized by high efficacy (E_{max} values), as compared with other $G_{q/11}$- or G_s-coupled receptors, respectively. Whereas R-q was devoid of agonist-independent (basal) signaling (Fig. S1*I*), R-s displayed a small degree of constitutive activity (*SI Appendix*, Fig. S1*J*).

Generation of Mutant Mice Expressing R-q and R-s in Pancreatic β Cells. Using standard transgenic techniques, we next generated mutant mice that specifically expressed R-q or R-s only in pancreatic β cells only (see *Materials and Methods* for details). We then selected two mouse lines that expressed similar numbers of R-q and R-s in their pancreatic islets for detailed phenotyping studies (number of [^{3}H]-NMS binding sites in fmol/mg membrane protein: R-q, 412 ± 109; R-s, 475 ± 35). These two mouse strains are hereafter referred to as β-R-q and β-R-s Tg mice. RT-PCR studies confirmed that R-q and R-s transcripts were not detectable in tissues other than pancreatic islets (*SI Appendix*, Fig. S3). All mutant and WT control mice used had a pure C57BL/6NTac background.

Initial Physiological Characterization of β-R-q and β-R-s Tg Mice. Initial phenotyping studies showed that growth curves, blood glucose levels, insulin sensitivity, and plasma insulin and glucagon levels were not significantly different between β-R-q Tg mice and their control littermates (*SI Appendix*, Fig. S4), indicating that the R-q receptor was devoid of ligand-independent signaling in vivo. A similar pattern was observed with β-R-s Tg mice, except that freely fed β-R-s Tg mice showed a significant decrease (by ≈20–25%) in blood glucose levels (compared to WT control mice) (*SI Appendix*, Fig. S4 *D* and *F*). This effect was not observed with fasted β-R-s Tg mice (*SI Appendix*, Fig. S4*I*).

The observation that freely fed β-R-s Tg mice showed reduced blood glucose levels may reflect the fact that the R-s receptor retained some degree of constitutive activity in vivo, consistent with the in vitro data (*SI Appendix*, Fig. S1*J*). Freely fed β-R-s Tg mice displayed normal plasma insulin levels (*SI Appendix*, Fig. S4*G*), and the presence of the β-R-s transgene had no effect on insulin sensitivity (*SI Appendix*, Fig. S4*E*). One possibility therefore is that constitutive signaling by R-s triggered increased insulin release in β-R-s Tg mice during times of feeding, resulting in reduced blood glucose levels. Whereas the increase in plasma insulin levels may be transient, effects on blood glucose levels may still persist even after insulin levels have returned to normal levels.

CNO Administration to β-R-q and β-R-s Tg Mice Induces Profound Dose-Dependent Hypoglycemic Effects. To determine the in vivo effects of acute activation of either β cell $G_{q/11}$ or G_s signaling on glucose homeostasis, we injected β-R-q and β-R-s Tg mice with increasing doses of CNO (0.0001–10 mg/kg i.p.) and monitored blood glucose levels for a 2-h period. All mice had free access to food until the beginning of the experiment and were kept fasting after CNO (or saline) administration. In both β-R-q and β-R-s Tg mice, CNO treatment resulted in a dose-dependent decrease in blood glucose levels (Fig. 2 *A* and *B*) and increased plasma insulin concentrations (*SI Appendix*, Fig. S5), demonstrating that the degree of β cell G protein signaling could be titrated according to the CNO dose administered. In general, the CNO-induced hypoglycemic and insulin-releasing effects were more pronounced in β-R-q than in β-R-s Tg mice.

To determine the duration of the CNO-induced hypoglycemic responses, freely fed β-R-q and β-R-s Tg mice were injected with CNO (1 mg/kg i.p.), and blood glucose levels were monitored over a 24-h period. Blood glucose levels were lowest at the 2 h time point and remained significantly reduced compared to preinjection values for at least 8 h in both mutant mouse lines (Fig. 2*C*).

To examine whether CNO was back-transformed into the parent drug, clozapine, we injected WT mice (C57BL/6NTac mice) with CNO (1 mg/kg i.p.) and collected blood samples for the measurement of CNO and clozapine plasma concentrations over a 2-h period. This analysis showed that no significant back-transformation of CNO to clozapine occurred during the entire observation period (*SI Appendix*, Fig. S6).

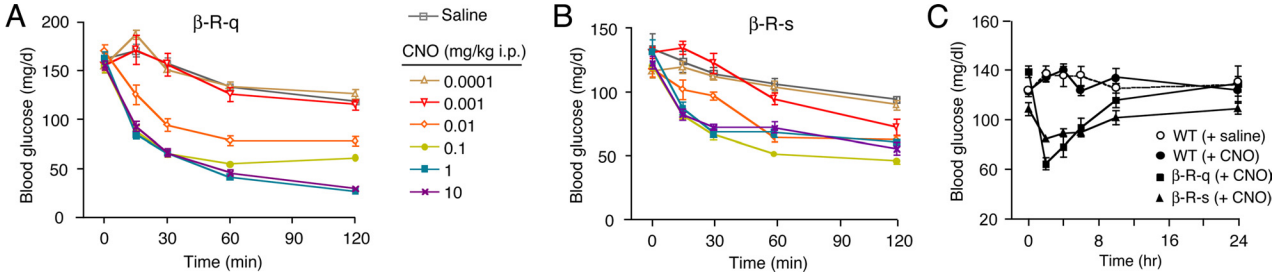

Fig. 2. Effect of CNO on blood glucose levels in β-R-q and β-R-s Tg mice. (*A* and *B*) Hypoglycemic effects following CNO administration in β-R-q and β-R-s Tg mice. β-R-q Tg (*A*) and β-R-s Tg mice (*B*) received a single i.p injection of increasing doses of CNO or vehicle (saline), and blood glucose levels were measured at the indicated time points. (*C*) Time course of the hypoglycemic effects of CNO. β-R-q and β-R-s Tg mice received a single dose of CNO (1 mg/kg i.p.), and blood glucose levels were monitored over a 24-h period. WT mice that had received either saline or the same dose of CNO served as controls. The data obtained with the two WT groups were pooled for the sake of clarity (no significant differences were found between these two groups). In all experiments, 3-month-old female mice with free access to food were used (five to eight mice per dose and/or group). Data are presented as means ± SEM.

Acute Activation of $G_{q/11}$ and G_s in β Cells Results in Marked Improvements in Glucose Tolerance Due to Greatly Enhanced Insulin Release. To assess the effects of acute activation of β cell $G_{q/11}$ or G_s signaling on glucose tolerance, we carried out i.p. glucose tolerance tests (IGTT) with β-R-q and β-R-s Tg mice, respectively. In both transgenic mouse lines, co-injection of CNO (1 mg/kg i.p.) with glucose (2 g/kg i.p.) resulted in a pronounced improvement in glucose tolerance (Fig. 3 *A* and *D*). In the case of β-R-q Tg mice, the CNO effect was so dramatic that no increases in blood glucose levels were observed at all at any of the indicated time points (Fig. 3*A*). In fact, CNO-treated β-R-q Tg mice became profoundly hypoglycemic at the 1 and 2 h time points (Fig. 3*A*).

To test the hypothesis that the CNO-induced improvements in glucose tolerance displayed by the β-R-q and β-R-s Tg mice were due to enhanced insulin release, we monitored changes in plasma insulin levels following co-injection of CNO (1 mg/kg i.p.) with glucose (2 g/kg i.p). Strikingly, co-injected β-R-q and β-R-s Tg mice showed pronounced increases in in vivo insulin release, as compared to transgenic mice that had received glucose alone (Fig. 3 *B* and *E*). Co-injected β-R-q Tg mice released approximately seven times more insulin over the 2-h observation period than β-R-q Tg mice injected solely with glucose (Fig. 3*C*). In contrast, co-injected β-R-s Tg mice released only approximately 2.5 times more insulin than β-R-s Tg mice that had received only glucose (Fig. 3*F*), consistent with the results of the glucose tolerance tests.

β-R-q and β-R-s Tg mice injected with glucose alone showed

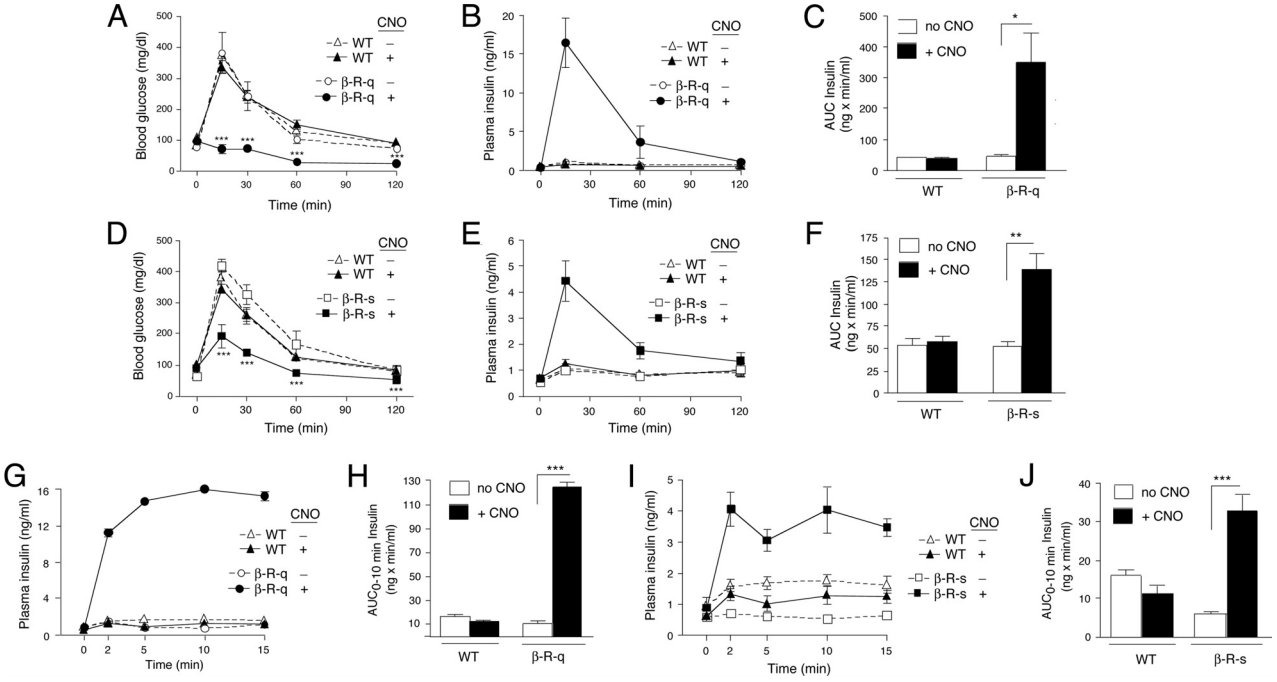

Fig. 3. Effect of CNO on glucose tolerance and insulin secretion in β-R-q and β-R-s Tg mice. (*A* and *D*) i.p. glucose tolerance test in β-R-q and β-R-s Tg mice and control littermates. Blood glucose levels were measured at the indicated time points following i.p. administration of glucose (2 g/kg). Glucose was injected either alone (-CNO) or together with CNO (1 mg/kg i.p.). (*B*, *C*, *E*, and *F*) Plasma insulin levels in glucose-injected β-R-q and β-R-s Tg mice and control littermates. Plasma insulin levels were measured at the indicated time points following i.p. administration of glucose (2 g/kg). Glucose was injected either alone (-CNO) or together with CNO (1 mg/kg i.p). In panels *C* and *F*, total insulin secretion from 0–120 min is expressed as area under the curve (AUC). (*G–J*) First-phase insulin release in glucose-injected β-R-q and β-R-s Tg mice and control littermates. Plasma insulin levels were measured immediately before (time 0) and 2, 5, 10, and 15 min after glucose administration (3 g/kg i.p.). Glucose was injected either alone or together with CNO (1 mg/kg i.p). In panels *H* and *J*, first-phase insulin release from 0–10 min is expressed as AUC. All experiments were carried out with 2- to 3-month-old female mice (five to seven mice per group). Data are presented as means ± SEM. *, $P < 0.05$; **, $P < 0.005$; ***, $P < 0.0005$, as compared to the corresponding non-CNO-treated Tg mouse group.

blood glucose and insulin excursions similar to the corresponding WT mice (Fig. 3 *A*, *B*, *D*, and *E*), indicating that basal (CNO-independent) signaling by R-s (*SI Appendix*, Fig. S1*J*) did not confound the outcome of the glucose tolerance and in vivo insulin release studies.

Given the importance of acute (first-phase) insulin release for proper glucose homeostasis (13, 14), we carried out additional in vivo insulin release experiments examining increases in plasma insulin levels in β-R-q and β-R-s Tg mice 2, 5, 10, and 15 min after glucose administration (3 g/kg i.p.). In these experiments, co-injection of CNO (1 mg/kg i.p.) with glucose led to a dramatic increase in in vivo insulin release at 2 min and all subsequent time points (Fig. 3 *G* and *I*). Co-injected β-R-q Tg mice released approximately 12 times more insulin over the first 10 min following CNO/glucose administration than β-R-q Tg mice injected with glucose alone (Fig. 3*H*). In contrast, co-injected β-R-s Tg mice released only approximately five times more insulin during this period than β-R-s Tg mice treated solely with glucose (Fig. 3*J*).

To examine the effects of CNO on first- and second-phase insulin secretion in more detail, we carried out in vitro insulin release studies using perifused islets prepared from β-R-q and β-R-s Tg mice. We found that CNO treatment (0.1 μM) of both β-R-q and β-R-s islets significantly enhanced both first- and second-phase insulin release in the presence of a high glucose concentration (16.7 mM) (*SI Appendix*, Figs. S7 and S8). In β-R-q islets, we noted a trend toward CNO-dependent increases in insulin secretion even at a low glucose concentration (2.8 mM). However, this effect was not consistently observed in all experiments (see legend to *SI Appendix*, Fig. S7). To further examine the effect of CNO on insulin release in β-R-q islets at a low ambient glucose concentration, we carried out additional insulin secretion studies using a static islet incubation assay. Under these experimental conditions, CNO (0.1 μM) had no significant effect on insulin release at 3.3 mM glucose, but triggered a profound increase in insulin secretion at 16.7 mM glucose, as expected (*SI Appendix*, Fig. S9). These data indicate that CNO does not consistently stimulate insulin release at low glucose concentrations in islets prepared from β-R-q mice.

The amount of insulin contained in pancreatic islets prepared from β-R-q and β-R-s Tg mice and WT control littermates (2-month-old females) did not differ significantly from each other (insulin content in ng/μg islet protein: WT, 29.1 ± 1.9; β-R-q, 40.3 ± 8.1; β-R-s, 44.5 ± 5.5; means ± SEM; three independent batches of islets from different groups of mice were tested per strain; $P > 0.05$). However, there was a clear trend toward an increase in islet insulin content in β-R-s Tg mice.

Studies with Obese, Insulin-Resistant β-R-q and β-R-s Tg Mice. An energy-rich, high-fat diet is known to trigger a number of metabolic changes including impaired glucose tolerance and insulin resistance. To examine to what extent acute activation of β cell $G_{q/11}$ or G_s signaling affected the severity of these metabolic disturbances, β-R-q and β-R-s Tg mice and their WT control littermates were fed a high-fat diet (HFD; fat content: 35.5%, wt/wt) and then monitored for a 12-week period. Expectedly, the transgenic mice and their WT control littermates maintained on the HFD gained significantly more weight than mice maintained on regular chow (RC) (*SI Appendix*, Fig. S10 *A* and *C*). This HFD-associated weight gain was accompanied by an approximately 3- to 5-fold increase in plasma insulin levels, as compared to mice maintained on RC (*SI Appendix*, Fig. S10 *B* and *D*), and greatly reduced insulin sensitivity, as shown in insulin tolerance tests (*SI Appendix*, Fig. S10*E*), indicative of an insulin-resistant state. Glucose tolerance tests (2 g glucose/kg i.p.) demonstrated that the HFD triggered glucose intolerance in WT and β-R-q Tg mice (*SI Appendix*, Fig. S10*F*). Strikingly, β-R-q Tg mice that had received CNO (1 mg/kg i.p.), together with the i.p glucose load, showed a dramatic improvement in glucose tolerance (*SI Appendix*, Fig. S10*F*), accompanied by a pronounced increase in in vivo insulin release (*SI Appendix*, Fig. S10*G*), as compared to β-R-q Tg mice treated with glucose alone. Co-injected β-R-q Tg mice exhibited an approximately 18-fold increase in total insulin release during the 2-h observation period, as compared with β-R-q Tg mice that had received only glucose (*SI Appendix*, Fig. S10*H*).

CNO (1 mg/kg i.p.) treatment of HFD β-R-s Tg mice led to qualitatively similar effects as described above for HFD β-R-q Tg mice (*SI Appendix*, Fig. S10 *I–K*). However, the CNO-dependent effects on glucose tolerance and in vivo insulin release were clearly less pronounced in HFD β-R-s Tg mice.

Morphometric Analysis of Pancreata from β-R-q and β-R-s Tg Mice. To examine the effect of chronic activation of either β cell $G_{q/11}$ or G_s signaling on β cell mass, mean islet size, and islet density, β-R-q and β-R-s Tg mice and WT control mice received daily injections of CNO (1 mg/kg i.p.) or saline (controls) for a 2-week period. Total pancreatic weights did not differ significantly among all groups studied (Fig. 4*A*).

In WT mice, CNO treatment had no significant effect on β cell mass, mean islet size, or islet density (Fig. 4 *B–D*). In contrast, CNO-treated β-R-q Tg mice showed an approximately 75% increase in β cell mass, as compared to saline-treated β-R-q Tg mice (saline, 0.8 mg ± 0.1 mg; CNO, 1.4 ± 0.1 mg; $P < 0.001$; Fig. 4*B*). This increase in β cell mass was accompanied by an approximately 60% increase in mean islet size in CNO-treated versus saline-treated β-R-q Tg mice (saline, 4,100 ± 400 μm^2; CNO, 6,600 ± 300 μm^2; $P < 0.001$; Fig. 4*C*). Islet density was similar in saline-treated and CNO-treated β-R-q Tg mice (Fig. 4*D*), suggesting that enlargement of existing islets is chiefly responsible for the increase in β cell mass observed with CNO-treated β-R-q Tg mice.

In contrast to saline-treated β-R-q Tg mice, saline-treated β-R-s Tg mice showed an approximately 160% increase in β cell mass, as compared to saline-treated WT mice (WT, 0.8 ± 0.1 mg; β-R-s, 2.1 ± 0.3 mg; $P < 0.0001$; Fig. 4*B*), consistent with the concept that basal R-s signaling triggers an increase in β cell mass. CNO treatment of β-R-s Tg mice did not lead to an additional increase in β cell mass (Fig. 4*B*). Unlike CNO-treated β-R-q Tg mice, both saline- and CNO-treated β-R-s Tg mice showed no significant changes in mean islet size, as compared to the corresponding WT control groups (Fig. 4*C*). However, in contrast to saline-treated β-R-q Tg mice, saline-treated β-R-s Tg mice exhibited an approximately 2-fold increase in islet density, as compared to saline-treated WT mice (WT, 1.2 ± 0.3 islets/mm^2; β-R-s, 2.5 ± 0.9 islets/mm^2; $P < 0.0001$; Fig. 4*D*). CNO-treated β-R-s Tg mice exhibited a similar increase in islet density, as compared to saline-treated or CNO-treated WT control mice (Fig. 4*D*), indicating that an increase in islet density is primarily responsible for the increase in β cell mass observed with β-R-s Tg mice. Representative images of pancreatic sections stained with an anti-insulin antibody are shown in *SI Appendix*, Fig. S11.

CNO treatment had no significant effect on the number of TUNEL-positive islet cells (a measure of cell apoptosis) in any of the mouse strains studied. However, CNO caused a significant increase in β cell (islet cell) size (by ≈15–30%) in both β-R-q Tg and β-R-s Tg mice (Fig. 4*E*). Taken together, these data suggest that the increase in β cell mass observed following β cell $G_{q/11}$ or G_s activation involves β cell hypertrophy and, possibly, an enhanced rate of β cell proliferation.

Islet Gene Expression Analysis. We next used real-time qRT-PCR to examine the effects of conditional β cell $G_{q/11}$ or G_s activation on the transcription of several genes important for β cell function and growth. To minimize the confounding effects of altered blood glucose levels on β cell (islet) gene expression (15), we carried out gene expression studies with freshly isolated islets cultured in the presence of a constant (physiological) concentration of glucose (5.5 mM). Islets were prepared from β-R-q and β-R-s Tg mice and WT control littermates and then treated with CNO (1 μM) at 37 °C for

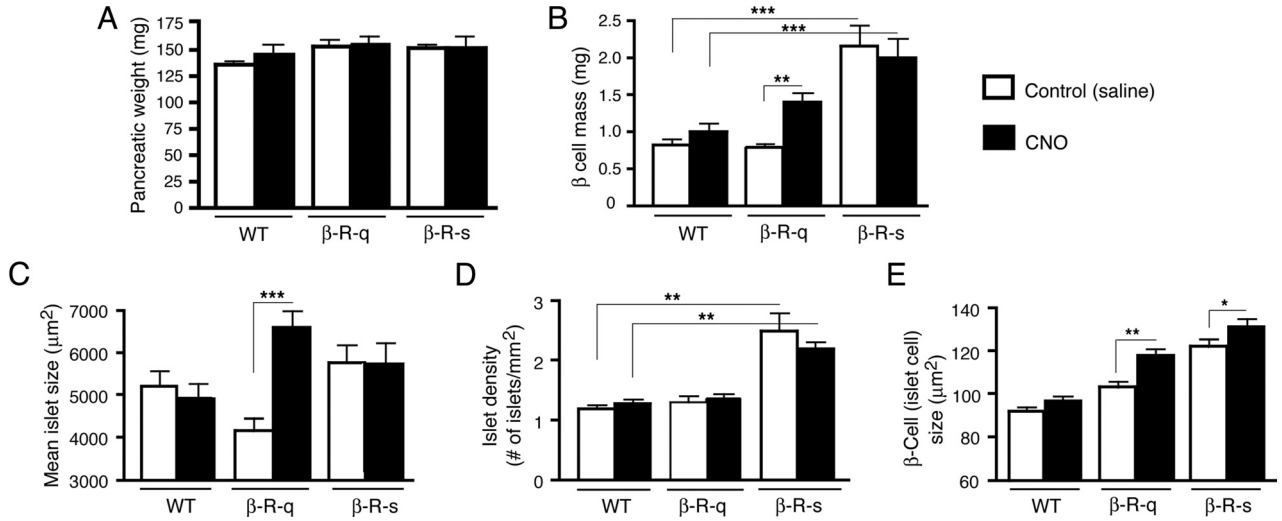

Fig. 4. Morphometric analysis of pancreata from β-R-q and β-R-s Tg mice and control littermates. β-R-q and β-R-s Tg mice and control littermates were treated for 2 weeks with daily injections of CNO (1 mg/kg i.p.) or saline (controls). (*A*) Total pancreatic weight (in mg). (*B*) β Cell mass (in mg). (*C*) Mean islet size (in μm^2). (*D*) Islet density (expressed as number of islets/mm^2 islet area). (*E*) β Cell (islet cell) size (in μm^2). All experiments were carried out with 2-month-old female mice (three to six mice per group; for details, see *Materials and Methods*). The data obtained with the two WT groups were pooled for the sake of clarity (no significant differences were found between these two groups). Data are presented as means ± SEM. *, $P < 0.05$, **, $P < 0.005$, ***, $P < 0.0005$.

3 h or left untreated (controls). Subsequently, total RNA was isolated and subjected to real-time qRT-PCR using validated primers. *SI Appendix*, Fig. S12 shows that CNO treatment of β-R-q Tg islets led to a small but significant increase in insulin (*Ins2*) and proprotein convertase 1 and 2 transcript levels ($P < 0.05$). A similar trend was also observed with CNO-treated β-R-s Tg islets. Most remarkably, CNO treatment of β-R-q Tg islets resulted in a pronounced (≈6-fold) increase in the levels of IRS-2 mRNA ($P < 0.0005$; *SI Appendix*, Fig. S12). A similar but quantitatively smaller increase in IRS-2 gene expression (≈2-fold) was also seen with CNO-treated β-R-s Tg islets ($P < 0.05$).

We also noted several pathway-specific changes in gene expression. Whereas CNO treatment of β-R-q Tg islets led to significantly reduced expression levels of Glut-2 and pyruvate carboxylase, no changes in the expression levels of these genes were observed with CNO-treated β-R-s Tg islets (*SI Appendix*, Fig. S12). On the other hand, CNO-treated β-R-s Tg islets showed a robust increase (≈4-fold) in acetyl-CoA carboxylase-2 (ACC2) gene expression levels, an effect that was not seen with CNO-treated β-R-q Tg islets (*SI Appendix*, Fig. S12).

We also examined the mRNA expression levels of several transcription factors and various other genes known to be important for β cell development and growth, including Pdx1, Neurog3, Nkx6–1, Neurod1, Mafa, Hnf4a, Ccnd1 (cyclin D1), Ccnd2 (cyclin D2), Cdk4, and Myc. However, under our experimental conditions, CNO treatment of β-R-q or β-R-s Tg islets failed to stimulate the expression of any of these genes.

Discussion

In this study, we used a chemical-genetic strategy to explore the in vivo consequences of selective and conditional activation of β cell $G_{q/11}$ or G_s signaling. Whereas the data obtained with the β-R-s Tg mice largely confirm previous results (5–7), the phenotypic analysis of β-R-q Tg mice has led to several important insights into the in vivo consequences of conditional and selective activation of β cell $G_{q/11}$ signaling. Moreover, since the R-q receptor, in contrast to the R-s construct, lacked ligand-independent signaling, the phenotypes displayed by the β-R-q Tg mice can be interpreted in a more straightforward fashion. Significantly, we demonstrated that selective activation of β cell $G_{q/11}$ signaling in vivo triggered a pronounced increase in first-phase insulin release, in addition to a long-lasting second phase of insulin release. This observation is of particular clinical relevance, since first-phase insulin release is considered critical for postprandial glucose homeostasis, and a reduction or loss of this response is a characteristic marker of β cell dysfunction in the early stages of type 2 diabetes (13, 14). Importantly, conditional and selective activation of β cell $G_{q/11}$ signaling in vivo also led to a striking improvement in glucose tolerance not only in mice consuming RC but also in obese, insulin-resistant mice.

We also made the observation that chronic, selective activation of β cell $G_{q/11}$ signaling resulted in a significant elevation in β cell mass, associated with an increase in mean islet size and β cell hypertrophy. Gene expression analysis demonstrated that conditional activation of β cell $G_{q/11}$ signaling triggered a robust increase in IRS-2 mRNA expression, probably due to $G_{q/11}$-mediated increases in intracellular Ca^{2+} levels (8, 16). Given the key role of IRS-2 in maintaining β cell function and mass (17, 18), it is likely that the observed increase in IRS-2 expression plays a major role in mediating the observed $G_{q/11}$-dependent increase in β cell mass. Clearly, more detailed mechanistic studies are needed to delineate the molecular pathways that link $G_{q/11}$ activation to increased IRS-2 expression and β cell mass. Gene expression analysis also showed that conditional activation of β cell $G_{q/11}$ signaling resulted in small but significant increases in insulin (*Ins2*) and proprotein convertase 1 and 2 transcript levels, suggesting that β cell $G_{q/11}$ signaling exerts a stimulatory effect on insulin synthesis.

The results obtained with the β-R-s Tg mice are largely consistent with previous studies suggesting that activation of β cell G_s improves β cell function, including an increase in β cell mass (5–7), thus representing a promising strategy to reduce pathologically elevated blood glucose levels. Consistent with this notion, exendin 4, which acts as an agonist at the G_s-coupled GLP-1 receptor, has been approved for the treatment of type 2 diabetes recently (5–7).

In general, the $G_{q/11}$-mediated in vivo metabolic effects were more pronounced than the corresponding G_s responses. However, a direct comparison between the effects observed with the two different mutant mouse strains is complicated by the fact that R-s showed some degree of agonist-independent signaling that may have triggered counter-regulatory responses in the β-R-s Tg mice. In agreement with this notion, Ma et al. (19) demonstrated that the expression of a constitutively active version of $G\alpha_s$ in β cells of

transgenic mice resulted in complex counter-regulatory effects. It is therefore conceivable that similar processes have occurred in β-R-s Tg mice, making a proper comparison between the in vivo phenotypes of the β-R-q and β-R-s Tg mice impossible. However, independent of these considerations, the robust, CNO-dependent in vivo phenotypes displayed by the β-R-q Tg mice strongly suggest that drugs that can enhance signaling through β cell $G_{q/11}$-coupled receptors may prove useful in the treatment of type 2 diabetes and glucose intolerance, similar to GLP-1 receptor agonists (5–7).

The use of engineered GPCRs with modified ligand binding properties to study various aspects of GPCR biology has been pioneered by Conklin and coworkers (20). However, in contrast to previous studies, the present in vivo study uses engineered GPCRs that are unable to bind endogenous ligand but can be efficiently activated by an otherwise pharmacologically inert drug.

In conclusion, the chemical-genetic approach described here has led to important insights into the functional roles of distinct G protein pathways in regulating β cell function in vivo. In principal, this technology can be applied to study the physiological and pathophysiological relevance of distinct G protein signaling pathways in virtually every cell type.

Materials and Methods

Drugs and WT Receptor Expression Constructs. Clozapine-N-oxide (CNO) was purchased from Biomol International. All other drugs were from Sigma-Aldrich. [^{3}H]N-methylscopolamine ([^{3}H]-NMS) and *myo*-[^{3}H] inositol were obtained from Perkin-Elmer Life and Analytical Sciences.

The mouse M3R coding sequence was cut out from a segment of cloned genomic DNA (21) and inserted into the pcD-PS mammalian expression vector. The mammalian expression vectors coding for the human V_2 vasopressin receptor (hV2-pcD-PS) (22) and the turkey β_1-adrenergic receptor have been described previously (β_1-pCMV) (23).

Generation of CNO-Sensitive Mutant M3Rs with Distinct G Protein Coupling Profiles. Mammalian expression plasmids coding for the R-q and R-s designer receptors (Fig. 1) were generated by standard molecular biological techniques (for details, see *SI Appendix*).

Transient Expression of Receptors in COS-7 Cells. COS-7 cells were grown as monolayers as described (24). For transfections, cells were plated at a density of 1×10^6 cells per 10-cm dish. About 24 h later, cells were transfected with 2 μg plasmid DNA using the Lipofectamine plus kit (Invitrogen).

[^{3}H]-NMS Radioligand Binding Assays. [^{3}H]-NMS saturation and inhibition binding assays were performed using membranes prepared from transfected COS-7 cells as described previously (24). ACh and CNO IC_{50} values were converted to K_i values using the Cheng-Prusoff equation.

Inositol Phosphate and cAMP Assays. Approximately 24 h after transfection, receptor-expressing COS-7 cells were placed into 6-well plates at a density of 1×10^6 cells/well. Cells were then incubated at 37 °C for 24 h with 1 μCi/mL *myo*-[^{3}H]inositol. Receptor-mediated increases in intracellular [^{3}H]-IP_1 levels were then determined as described (24). In a similar fashion, receptor-mediated increases in intracellular cAMP assays were measured via ELISA according to the manufacturer's protocol (cAMP; Biotrak; Amersham Biosciences).

Generation of Transgenic Mice and Mouse Maintenance and Diet. Mutant mice selectively expressing the R-q and R-s mutant receptors in their pancreatic β cells were obtained by using standard transgenic techniques (for details, see *SI Appendix*). All mouse lines were maintained on a pure C57BL/6NTac background. Mouse genotyping and RT-PCR analysis of transgene expression were carried out as described under *SI Appendix*.

Unless noted otherwise, 2- to 4-month-old female or male mice were used for phenotyping studies. Mice were fed ad libitum and kept on a 12-h light, 12-h dark cycle. For diet-induced obesity studies, mice were fed a diet containing 35.5% calories from fat (product no. F3282; BioServ). All experiments were approved by the Animal Care and Use Committee of the National Institute of Diabetes and Digestive and Kidney Diseases, NIH, Bethesda, MD.

Physiological Studies. Glucose and insulin tolerance tests were carried out after an overnight fast (10–12 h), and plasma insulin and glucagon levels were determined via ELISA, as described in detail previously (9).

Islet Binding Assays and Determination of Islet Insulin Content. R-q and R-s expression levels in membrane preparations prepared from isolated islets of β-R-q and β-R-s Tg mice were quantitated in radioligand binding studies as described previously (9), using a saturating concentration of [^{3}H]-NMS (20 nM; three to four mice per strain per experiment). Islet insulin content was measured by using an acid-ethanol method, as described previously (9). For each mouse strain, three to four separate batches of islets (30 islets per batch) were prepared from three to four different mice.

Morphometric Analysis of Pancreatic Islets. Islet morphometric studies were performed with 8-week-old female mice (three mice per strain and treatment group) by using standard techniques (for details, see *SI Appendix*).

Real-Time qRT-PCR Analysis of Islet Gene Expression. Total RNA was prepared from pancreatic islets of β-R-q and β-R-s Tg mice and WT littermates (three to four mice per strain per experiment). Subsequently, gene expression levels were determined via real-time qRT-PCR (for details, see *SI Appendix*).

Statistics. Data are expressed as means ± SEM or SD for the indicated number of observations. For comparisons between two groups, the unpaired Student's *t*-test (two-tailed) was used. For multiple comparisons, the one-way analysis of variance (ANOVA) was used. A P value of <0.05 was considered statistically significant.

ACKNOWLEDGMENTS. We thank Ms. Xiaohong Zhang and Ms. Yinghong Cui for excellent technical assistance; Dr. Elliot Ross (UT Southwestern Medical Center, Dallas, TX) for providing the turkey β_1-adrenergic receptor expression vector; The National Institutes of Health Inter-institute Endocrine Training Program, particularly Drs. M.C. Skarulis, L.K. Nieman, D. LeRoith, and P. Gorden for support of this work. This work was supported by the Intramural Research Program, the National Institute of Diabetes and Digestive and Kidney Diseases, National Institutes of Health; U.S. Department of Health and Human Services; and National Institutes of Health Grants U19MH82441, NO1MH80004, and RO1MH61887.

1. Zimmet P, Alberti KG, Shaw J (2001) Global and societal implications of the diabetes epidemic. *Nature* 414:782–787.
2. Kahn CR (1994) Insulin action, diabetogenes, and the cause of type II diabetes (Banting Lecture). *Diabetes* 43:1066–1084.
3. Regard JB, et al. (2007) Probing cell type-specific functions of G_i in vivo identifies GPCR regulators of insulin secretion. *J Clin Invest* 117:4034–4043.
4. Regard JB, Sato IT, Coughlin SR (2008) Anatomical profiling of G protein-coupled receptor expression. *Cell* 135:561–571.
5. Ahrén B (2009) Islet G protein-coupled receptors as potential targets for treatment of type 2 diabetes. *Nat Rev Drug Discov* 8:369–385.
6. Doyle ME, Egan JM (2007) Mechanisms of action of glucagon-like peptide 1 in the pancreas. *Pharmacol Ther* 113:546–593.
7. Baggio LL, Drucker DJ (2007) Biology of incretins: GLP-1 and GIP. *Gastroenterology* 132:2131–2157.
8. Gilon P, Henquin JC (2001) Mechanisms and physiological significance of the cholinergic control of pancreatic β-cell function. *Endocr Rev* 22:565–604.
9. Gautam D, et al. (2006) A critical role for β cell M_3 muscarinic acetylcholine receptors in regulating insulin release and blood glucose homeostasis in vivo. *Cell Metab* 3:449–461.
10. Steneberg P, Rubins N, Bartoov-Shifman R, Walker MD, Edlund H (2005) The FFA receptor GPR40 links hyperinsulinemia, hepatic steatosis, and impaired glucose homeostasis in mouse. *Cell Metab* 1:245–258.
11. Armbruster BN, Li X, Pausch MH, Herlitze S, Roth BL (2007) Evolving the lock to fit the key to create a family of G protein-coupled receptors potently activated by an inert ligand. *Proc Natl Acad Sci USA* 104:5163–5168.
12. Alexander GM, et al. (2009) Remote control of neuronal activity in transgenic mice expressing evolved G protein-coupled receptors. *Neuron* 63:27–39.
13. Del Prato S, Marchetti P, Bonadonna RC (2002) Phasic insulin release and metabolic regulation in type 2 diabetes. *Diabetes* 51(Suppl 1):S109–S116.
14. Nesher R, Cerasi E (2002) Modeling phasic insulin release: Immediate and time-dependent effects of glucose. *Diabetes* 51(Suppl 1):S53–S59.
15. Ohsugi M, et al. (2004) Glucose and insulin treatment of insulinoma cells results in transcriptional regulation of a common set of genes. *Diabetes* 53:1496–1508.
16. Lingohr MK, et al. (2006) Specific regulation of IRS-2 expression by glucose in rat primary pancreatic islet β-cells. *J Biol Chem* 281:15884–15892.
17. Niessen M (2006) On the role of IRS2 in the regulation of functional β-cell mass. *Arch Physiol Biochem* 112:65–73.
18. White MF (2006) Regulating insulin signaling and β-cell function through IRS proteins. *Can J Physiol Pharmacol* 84:725–737.
19. Ma YH, et al. (1994) Constitutively active stimulatory G-protein α_s in β-cells of transgenic mice causes counterregulation of the increased adenosine 3′,5′-monophosphate and insulin secretion. *Endocrinology* 134:42–47.
20. Conklin BR, et al. (2008) Engineering GPCR signaling pathways with RASSLs. *Nat Methods* 5:673–678.
21. Yamada M, et al. (2001) Mice lacking the M3 muscarinic acetylcholine receptor are hypophagic and lean. *Nature* 410:207–212.
22. Schöneberg T, Yun J, Wenkert D, Wess J (1996) Functional rescue of mutant V2 vasopressin receptors causing nephrogenic diabetes insipidus by a co-expressed receptor polypeptide. *EMBO J* 15:1283–1291.
23. Wong SK, Parker EM, Ross EM (1990) Chimeric muscarinic cholinergic:β-adrenergic receptors that activate G_s in response to muscarinic agonists. *J Biol Chem* 265:6219–6224.
24. Han SJ, et al. (2005) Pronounced conformational changes following agonist activation of the M_3 muscarinic acetylcholine receptor. *J Biol Chem* 280:24870–24879.